Supplementary Information for

Gut Flora Disequilibrium Promotes the Initiation of Liver Cancer by Modulating Tryptophan Metabolism and Upregulating SREBP2

Wen Chen, Liang Wen, Yingying Bao, Zengwei Tang, Jianhui Zhao, Xiaozhen Zhang, Tao Wei, Jian Zhang, Tao Ma, Qi Zhang, Xiao Zhi, Jin Li, Cheng Zhang, Lei Ni, Muchun Li and Tingbo Liang*

*Corresponding Author: Tingbo Liang, E-mail: liangtingbo@zju.edu.cn

This PDF file includes:

Materials and methods

Bacteria 16s rRNA Sequencing

Stool samples were collected from mice after 14 days of treatment with ABX or H_2O, snap-frozen in liquid nitrogen, and stored at -80 ℃. Fecal total genomic DNA was extracted using the CTAB (Cetyltrimethylammonium Bromide) method. The 16s V3-V4 region was amplified using primers 341F CCTAYGGGRBGCASCAG and 806R GGACTACNNGGGTATCTAAT with barcodes. The PCR products were mixed at equal densities and purified using a Qiagen Gel Extraction Kit (Qiagen, Hilden, Germany). Sequencing libraries were generated using a TruSeq DNA PCR-Free Sample Preparation Kit (Illumina, San Diego, CA, USA). The quality of the library was assessed on a Qubit 2.0 Fluorometer (Thermo Fisher Scientific) and an Agilent Bioanalyzer 2100 system. Sequencing of the library was performed on an Illumina NovaSeq6000 platform (Novogene, Beijing, China) and 250 bp paired-end reads were generated. Paired-end reads were assigned to samples based on their barcodes and truncated by cutting off the barcode and primer sequence. Paired-end reads were then merged using FLASH (V1.2.7) to obtain the raw tags (1). The raw tags were filtered to obtain high quality clean tags using fastp (Version 0.20.0) quality control process (2). After removing the chimeric sequences detected by comparing tags with the Silva database using Vsearch (Version 2.15.0) algorithm, the effective tags were obtained. Then, denoise was performed with DADA2 in the QIIME2 software (Version QIIME2-202006) to obtain initial ASVs (Amplicon Sequence Variants), ASVs with abundance less than 5 were filtered out (3). Taxonomic information was annotated using the Silva database by QIIME2 software. Using a standard sequence number corresponding to the sample with the least sequences to normalize the absolute abundance of ASVs. Subsequent analysis of alpha diversity and beta diversity were all performed based on the normalized data.

Tissue mRNA Sequencing

Total RNA was extracted from liver tissues using the Trizol reagent (Invitrogen). Degradation and contamination of the RNA was monitored on 1% agarose gels. RNA purity was checked using a NanoPhotometer spectrophotometer (IMPLEN, CA, USA). The quality of the RNA was assessed using a Bioanalyzer 2100 system with an RNA Nano 6000 Assay Kit (Agilent Technologies, CA, USA). Sequencing libraries were prepared with an NEBNext Ultra™ RNA Library Prep Kit for Illumina (NEB,

USA) following the manufacturer's recommendations. Index codes were added to attribute the sequences to each sample. The sequencing library was purified using the AMPure XP system and library quality was assessed on the Agilent Bioanalyzer 2100 system. Sequencing of the library was performed on an Illumina NovaSeq6000 platform (Novogene) and 150 bp paired-end reads were generated. Clean reads were obtained by removing reads containing adapters, poly-N, and low-quality reads from the raw reads and subsequent analyses were based on the clean reads. Paired-end clean reads were aligned to the mouse reference genome using Hisat2 v2.0.5. Quantification of gene expression was performed using FeatureCounts v1.5.0-p3 to obtain the read numbers mapped to each gene and then the FPKM (fragments per kilobase of transcript per million mapped reads) of each gene was calculated. Differential expression analysis of the ABX and control groups was performed using the DESeq2 R package (1.16.1). Pathway enrichment analysis was performed by Gene Ontology and Reactome database analysis using the R package, clusterProfiler.

Detection of Tryptophan and Its Metabolites

Stool samples were collected from mice in the indicated groups, snap-frozen in liquid nitrogen, and then stored at -80℃. A 50 mg sample was weighted, thawed, and extracted using 500 μL of methanol. 20 μL of an internal standard mixed solution (250 ng/mL) was added to the extract as internal standards for quantification. The extract was vortexed for 3 min and then incubated at -20 °C for 30 min. The extract was centrifuged at 12000×rpm for 10 min at 4 °C, and 250 μL of the supernatant was collected. The supernatant was centrifuged again at 12000×rpm for 5 min at 4 °C. Tryptophan and its metabolites contents were then detected by MetWare Biotechnology Co., Ltd (Wuhan, China) based on a previously described protocol (4). The sample extracts were analyzed using an LC-ESI-MS/MS system (UPLC, ExionLC AD, https://sciex.com.cn/; MS, QTRAP® 6500+ System, https://sciex.com/). Linear ion trap and triple quadrupole scans were acquired on a triple quadrupole-linear ion trap mass spectrometer (QTRAP), QTRAP® 6500+ LC-MS/MS System, equipped with an ESI Turbo Ion-Spray interface, operating in both positive and negative ion mode and controlled by Analyst 1.6.3 software (Sciex). The ESI source operation parameters were as follows: ion source, ESI+/-; source temperature 550 ℃; ion spray voltage 5500 V (Positive), -4500 V (Negative); curtain gas was set at 35 psi, respectively. Tryptophan and its metabolites were analyzed using scheduled multiple reaction monitoring. Data acquisitions were performed using Analyst 1.6.3 software (Sciex). Multiquant 3.0.3 software (Sciex) was

used to quantify all the metabolites. PCA was performed by statistics function prcomp within R. Significantly regulated metabolites between groups were determined by VIP (variable importance in projection) ≥ 1 and absolute Log2FC (fold change) ≥ 1.0 (fold change ≥ 2). Variable importance in projection (VIP) values were extracted from the orthogonal projections to latent structures discriminant analysis (OPLS-DA) results, which also contain score plots and permutation plots, were generated using R package MetaboAnalystR.

Immunoblotting

Liver samples were collected from mice in the indicated groups, snap-frozen in liquid nitrogen, and stored at -80 ℃. Liver tissues were weighted (30 mg) and homogenized in 300 μl of radioimmunoprecipitation assay (RIPA) buffer (Beyotime Biotechnology, catalog # P0013B) containing a protease inhibitor cocktail (Roche, catalog # 05056489001), followed by centrifugation at 12000×*g* for 15 min. The supernatant was collected and the protein concentration was measured using the bicinchoninic acid (BCA) reagent (Beyotime Biotechnology, catalog # P0012). Equal amounts of protein were separated using 8% sodium dodecyl sulfate–polyacrylamide gels and transferred to polyvinylidene fluoride membranes (Millipore). Vinculin was monitored as the internal control. The primary antibodies recognized: SREBP2 (Santa Cruz Biotechnology, catalog # sc-13552), HMGCR (Santa Cruz Biotechnology, catalog # sc-271595), HMGCS1 (Abcam, catalog # ab155787), FDFT1 (Abcam, catalog # ab195064), SQLE (Proteintech, catalog # 12544-1-AP), AHR (Enzo Life Science, catalog # BML-SA210), and Vinculin (Abcam, catalog # ab129002). The secondary antibodies comprised: anti-rabbit IgG, HRP-linked antibody (Beyotime Biotechnology, catalog # A0208) and anti-mouse IgG, HRP-linked antibody (Beyotime Biotechnology, catalog # A0216). The immunoreactive signals were detected using an EzWay DAB Western Blot Kit (KOMA BIOTECH, Seoul, Korea) and were visualized using ChemiScopeTouch (Clinx Science Instruments, Shanghai, China).

Quantitative Real-Time Reverse Transcription-PCR Analysis

Total RNA was extracted from liver tissues using the Trizol reagent (Invitrogen) and the RNA concentration was measured using a NanoDrop One spectrophotometer (Thermo Scientific). cDNA synthesis was performed using a PrimeScript RT reagent kit (Takara catalog, # RR047A). The

quantitative real-time PCR step was performed using the Applied Biosystems 7500 Fast Real-Time PCR System with TB Green (Takara catalog, # RR820A). The relative gene expression levels were normalized to that of *Rps18* and calculated using 2−ΔΔCt method as previously described (5). Primer sequences were as follows: *Srebf2* (Forward: GATGAGCTGACTCTCGGGGACATC, Reverse: GTGGGGTAGGAGAGACTTTGACCT); *Sqle* (Forward: CGCAGCGGTTACTCTGGTTA, Reverse: ATTCCTCCTCAAGCAAGCCC); *Lss* (Forward: GCTGTCAGGTAAAGGGCTGG, Reverse: CTGCCGACCCAACTCATTCT); *Idi1* (Forward: TGGGGCTGACACCAAGAAAA, Reverse: CTTTGCTGCTCGCTTCACAC); *Hmgcr* (Forward: GGTGCAAAGTTCCTTAGTGATG, Reverse: GAATAGACACACCACGTTCATG); *Hmgcs1* (Forward: GGTTGGAGTGTTCTCTTACGGTTCTG, Reverse: GATCCTGGTGTGGCGTCTTGTG); *Fdtf1* (Forward: ATGGAGTTCGTCAAGTGTCTAG, Reverse: ACCAGGTAGAACACACATATGG); *Cyp1a1* (Forward: CAGGATGTGTCTGGTTACTTTGAC, Reverse: CTGGGCTACACAAGACTCTGTCTC). Rps18 primers were bought from Shanghai Sangon Biotech (catalog # B661301).

Measurements of Plasma and Liver Parameters

Blood samples were collected into heparin-coated tubes and centrifuged at 3000×*g* for 15 min. Liver samples were homogenized in saline and centrifuged at 3000×*g* for 10 min. The supernatants of the blood and liver samples were collected and stored at -80 ℃ for further analysis. Supernatant measurements of cholesterol, triglycerides, aspartate transaminase (AST), alanine transaminase (ALT), total bilirubin (TBIL), and total bile acids (TBA) were performed using a Chemray 800 Automatic Biochemical Analyzer (Rayo Science, Shenzhen, China).

Liver Histology and Immunohistochemistry

The left lobe of the liver was stored in 10% neutral buffered formalin, embedded in paraffin, sectioned into 4 μm slices, mounted on a super frost glass slide, and stained with hematoxylin and eosin (H&E). For immunohistochemical staining (IHC), the primary antibodies recognized Ki67 (Cell Signaling Technology, catalog # 12202) and anti-rabbit IgG, HRP-linked antibodies (Beyotime Biotechnology, catalog # A0208) were used as the secondary antibody. The slides were dewaxed, and the antigen was retrieved by boiling the slides in citrate buffer (Solarbio Life Science) for 10 min and then cooled at room temperature for 30 min. The slides were blocked with 3% bovine serum albumin for

30 min at room temperature and incubated with Ki67 antibody overnight at 4 °C. Then, the slides were washed with PBS and incubated with secondary anti-rabbit IgG antibody for 20 min at room temperature. The chromogen reaction was performed using a diaminobenzidine (DAB) chromogen kit (Biocare, catalog # BDB2004). The slides were counterstained with hematoxylin for 3-5 min. Representative images of samples were captured using ImageScope software (Leica Biosystems).

Flow Cytometric Analysis.

Samples were cut in small fragments with scissors and then digested in Dulbecco's modified Eagle's medium (DMEM) supplemented with 1% fetal bovine serum (FBS), collagenase IV (1 mg/ml) (Thermo Fisher Scientific, catalog # 17104019), DNase (10 μg/ml) (Sigma-Aldrich, catalog # D5025), Dispase (0.6 mg/ml) (Gibco, catalog # 17105041), and $CaCl_2$ (3 mM) (Sigma-Aldrich, catalog # 21115) with shaking at 200 rpm for 20 min at 37 °C, and then forced through a 40-μm cell strainer (Thermo Fisher Scientific, catalog # 08-771-1). A 36% Percoll solution (GE Healthcare) containing 4% 10×PBS and 60% DMEM were used to remove non-immune cells. RBC lysis buffer (BD Biosciences) was used to lyse red blood cells. Cells were blocked using TruStain FcX™ (an anti-mouse CD16/32 antibody) then stained with the indicated antibodies. Flow cytometry was performed on the Beckman CytoFLEX LX platform and the results were analyzed using FlowJo software. Monoclonal antibodies recognizing the following proteins were used for flow cytometry analysis: CD45 (BD Biosciences, catalog # 752409), CD3 (Biolegend, catalog # 00203), CD4 (Biolegend, catalog # 100413), CD8 (Biolegend, catalog # 100744), CD19 (BD Biosciences, catalog # 563557), CD49b (Biolegend, catalog # 103516), CD11b (BD Biosciences, catalog # 562399), F4/80 (Biolegend, catalog # 123114), CD11c (Biolegend, catalog # 301610), MHCII (Biolegend, catalog # 107632), and 7AAD (BD Biosciences, catalog # 559925).

Human studies

Fecal samples and liver tissue samples were obtained from the Department of Hepatobiliary and Pancreatic Surgery, the First Affiliated Hospital, School of Medicine, Zhejiang University. All human studies were approved by the Institutional Review Board at the First Affiliated Hospital, School of Medicine, Zhejiang University. The inclusion criteria for HCC patients were as follows: 1) first diagnosed with primary HCC without other tumor occurrences; 2) patients did not receive any treatment for HCC before fecal samples collection; 3) patients did not receive any antibiotics during 6 months

before sampling. The inclusion criteria of healthy persons (fecal samples collection) were as follows: 1) healthy subjects had no prior history of malignancy or other major illness; 2) healthy subjects did not receive any antibiotics during 6 months before sampling. The procedures of fecal bacteria 16s rRNA sequencing and tryptophan metabolites detection were the same as mentioned above. As for significantly regulated tryptophan metabolites in human subjects were determined by VIP (variable importance in projection) ≥ 1 and absolute Log2FC (fold change) ≥ 0.58 (fold change ≥ 1.5). HCC tissues and matched adjacent non-tumor tissues from HCC patients who underwent surgical resection were obtained for q-rtPCR and immunoblotting. The *Cyp1a1* expression level was normalized to that of *Actb* and calculated by $2^{-\Delta Ct}$, and comparisons between HCC tissues and matched adjacent non-tumor tissues were performed using two-tailed paired t test. Primer sequences were as follows: *Cyp1a1* (Forward: CTTCCGACACTCTTCCTTCG, Reverse: GGTTGATCTGCCACTGGTTT); *Actb* (Forward: CTCGCCTTTGCCGATCC, Reverse: TCTCCATGTCGTCCCAGTTG). For immunoblotting, the primary antibody SREBP2 (Novus, catalog # NBP1-71880) was used for human samples and Vinculin (Abcam, catalog # ab129002) was monitored as the internal control.

Supplementary figures and figure legends

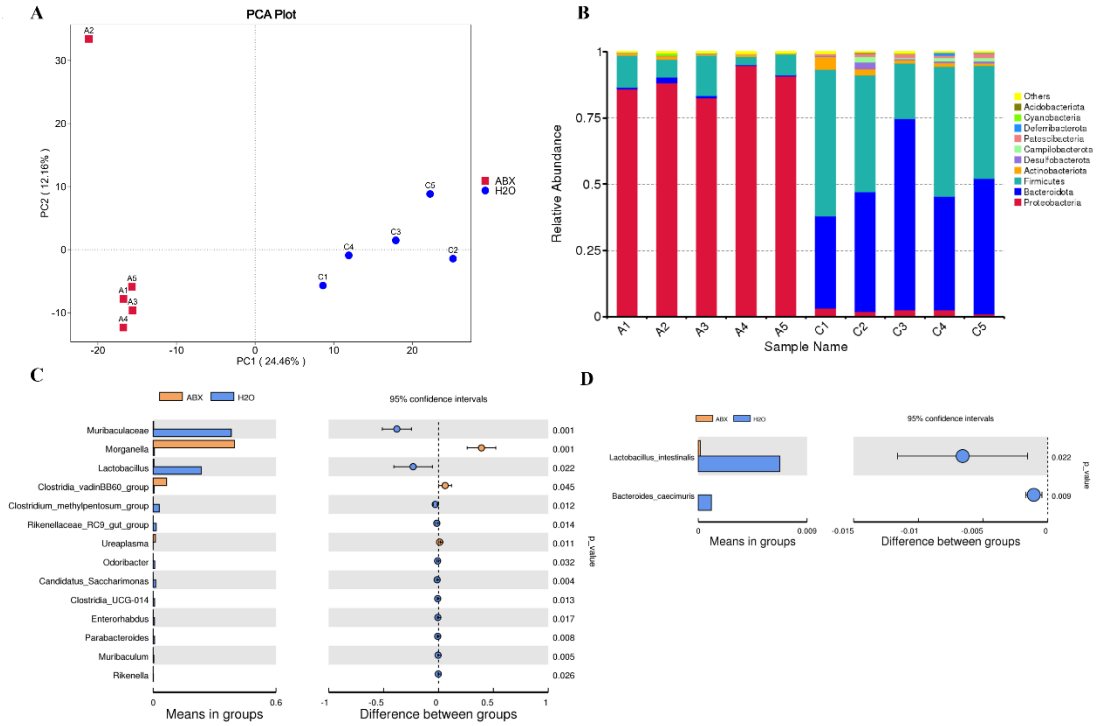

Fig. S1 Gut flora disequilibrium induced by antibiotics treatment.

(A) PCA of 16S rRNA sequencing data from ABX or H_2O fed mice feces (n = 5 per group). (B) Taxonomic distribution of the fecal microbiome. Fecal bacteria proportion at the phylum level and the top 10 taxa are annotated on the right. (C) Beta-diversity comparison at the genus level based on t-test significance results. (D) Beta-diversity comparison at the species level based on t-test significance results.

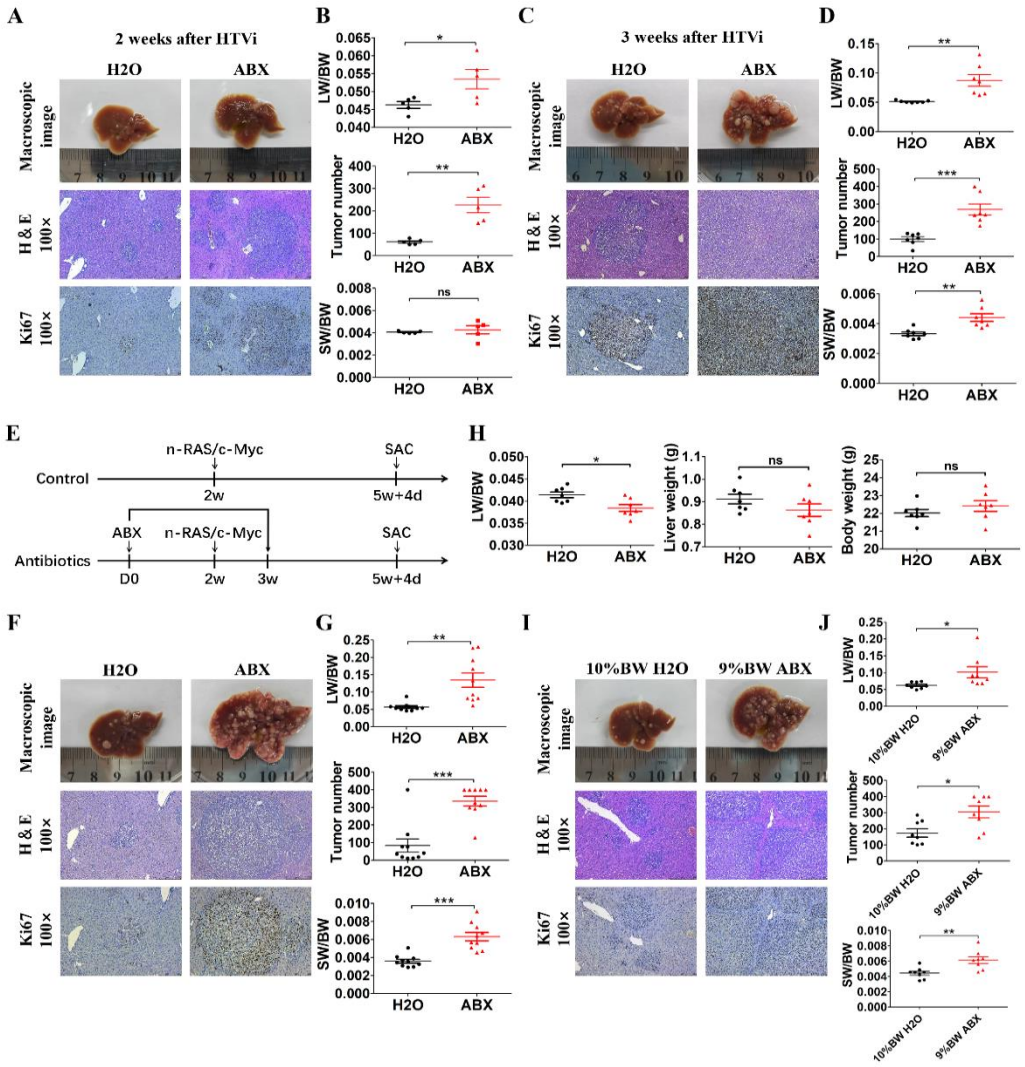

Fig. S2 Gut commensal bacteria depletion promoted liver tumor initiation under different conditions.

(A) Mice were transfected with n-Ras/c-Myc by HTVi at 2 weeks after the administration of ABX or H_2O and sacrificed 2 weeks after oncogene injection. Representative macroscopic views of livers, H&E staining, and IHC of Ki67 in mouse HCCs. (B) The liver-body weight ratio (LW/BW), tumor number, and the spleen-body weight ratio (SW/BW) of each group (n = 5 per group). (C) Mice were transfected with n-Ras/c-Myc by HTVi at 2 weeks after the administration of ABX or H_2O and sacrificed 3 weeks after oncogene injection. Representative macroscopic views of livers, H&E staining, and IHC of Ki67 in mouse HCCs. (D) The liver-body weight ratio (LW/BW), tumor number, and the spleen-body weight ratio (SW/BW) of each group (n = 7 per group). (E) Experimental procedure. Mice were transfected with N-Ras/c-Myc by HTVi at 2 weeks after the administration of ABX or H_2O, ABX was removed 1 week after HTVi, and mice were sacrificed 25 days after oncogene injection. (F) Representative macroscopic views of livers, H&E staining, and IHC of Ki67 in mouse HCCs. (G) The liver-body weight ratio (LW/BW), tumor number, and the spleen-body weight ratio (SW/BW) of each group (n = 10 per group). (H) Liver-body weight ratio (LW/BW), liver weight, and body weight of mice with 14 days of ABX or H_2O treatment. (I) Mice were transfected with 0.09 mL/g body weight volume of PBS (Ras/Myc) at 2 weeks after the administration of ABX and control mice were transfected with 0.1 mL/g body weight volume of PBS (Ras/Myc) by HTVi; mice were sacrificed 4 weeks after oncogene injection. Representative macroscopic views of livers, H&E staining, and IHC of Ki67 in mouse HCCs. (J) The liver-body weight ratio (LW/BW), tumor number, and the spleen-body weight ratio (SW/BW) of each group (n = 8 per group). Data was presented as mean ± SEM, *P* values were calculated by Student' s t-test. ns, not significant; **P* <0.05; ***P* <0.01; ****P* <0.001.

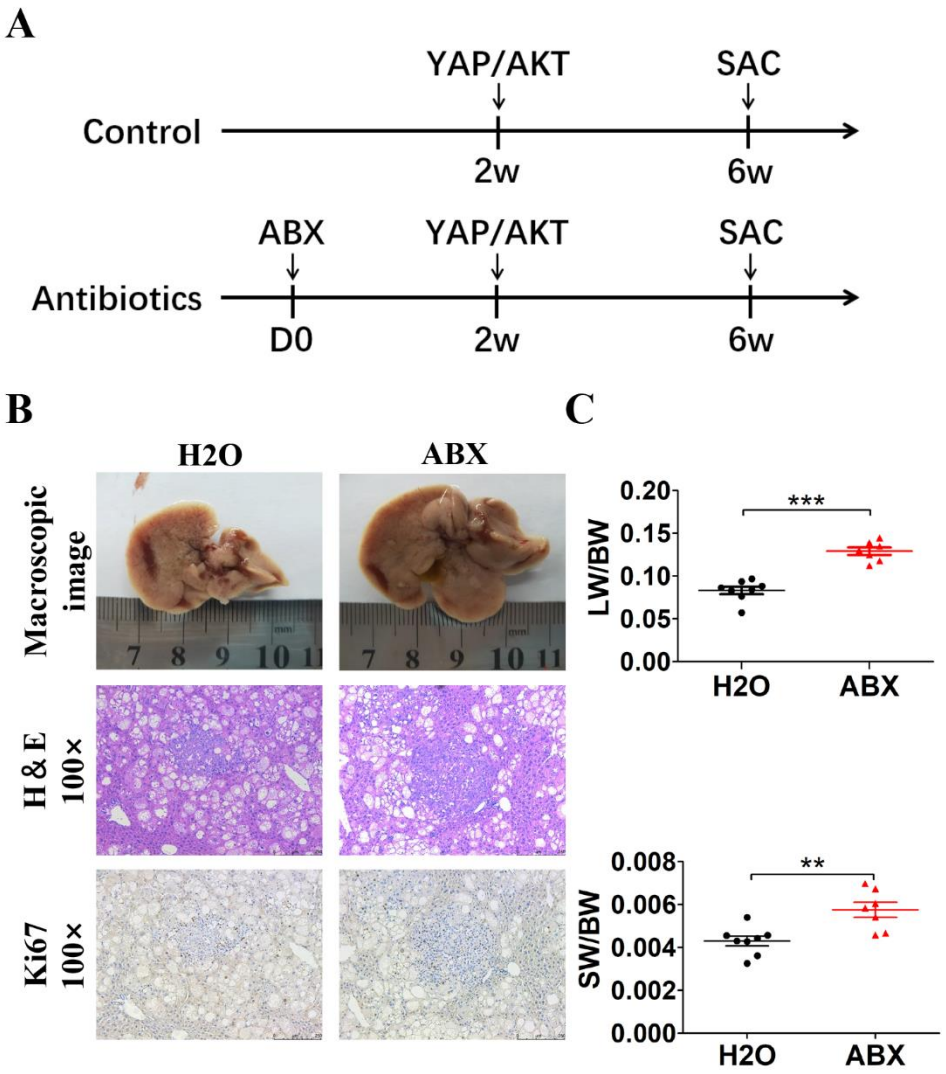

Fig. S3 Gut commensal bacteria depletion promoted intrahepatic cholangiocarcinoma (ICC) initiation in mice.

(A) Experimental procedure (H_2O n=8; ABX n=7). (B) Representative macroscopic views of livers, H&E staining, and IHC of Ki67 in mouse ICCs. (C) The liver-body weight ratio (LW/BW) and the spleen-body weight ratio (SW/BW) of each group. Data was presented as mean ± SEM, *P* values were calculated by Student' s t-test. ***P* <0.01; ****P* <0.001.

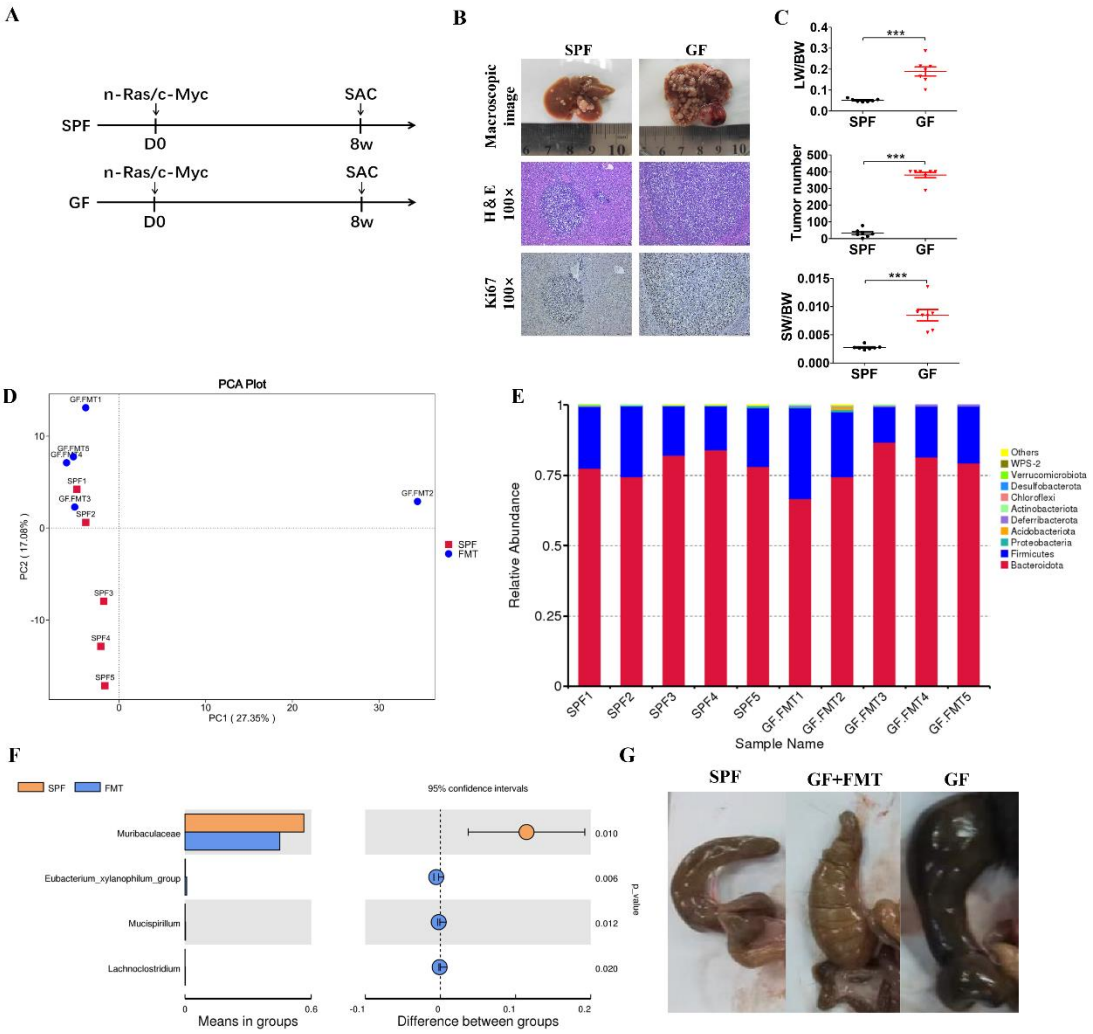

Fig. S4 GF status promoted liver tumor initiation and FMT reconstituted the gut microbiota composition in GF mice.

(A) Experimental procedure. GF and SPF mice were transfected with 0.07 mL/g body weight volume of PBS (Ras/Myc) by HTVi and were sacrificed 8 weeks after oncogene injection. (B) Representative macroscopic views of livers, H&E staining, and IHC of Ki67 in mouse HCCs. (C) The liver-body weight ratio (LW/BW), tumor number, and the spleen-body weight ratio (SW/BW) of each group (n = 7 per group). (D) PCA of 16S rRNA sequencing data from SPF or GF+FMT mice feces (n = 5 per group). (E) Taxonomic distribution of the fecal microbiome. Fecal bacteria proportion at the phylum level and the top 10 taxa are annotated on the right. (F) Beta-diversity comparison at the genus level based on t-test significance results. (G) Reduced cecum volume of GF mice after FMT from SPF mice. Data was presented as mean ± SEM, *P* values were calculated by Student's t-test. ***P <0.001.

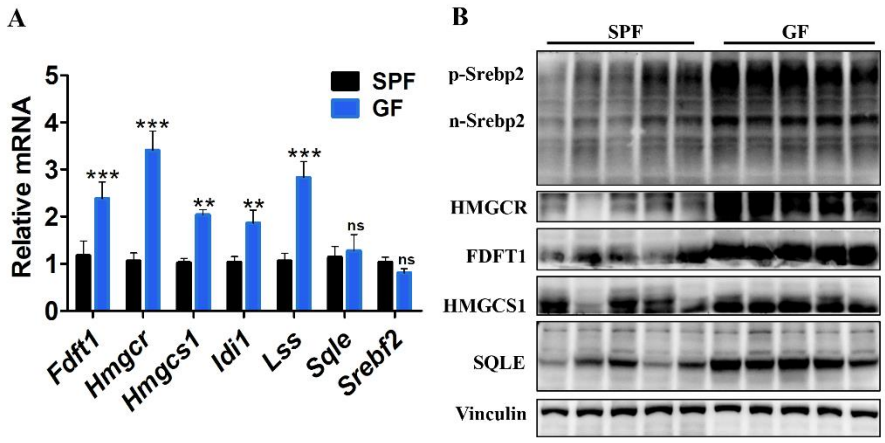

Fig. S5 SREBP2 and downstream cholesterol synthesis related gene expression increased in GF mice.

(A) Gene expression in liver tissues from GF and SPF mice were determined by qRT-PCR (n = 5 per group). (B) Western blotting analysis of liver tissues from GF and SPF mice (n = 5 per group). Data was presented as mean ± SEM, *P* values were calculated by Student' s t-test. ns, not significant; ***P* <0.01; ****P* <0.001.

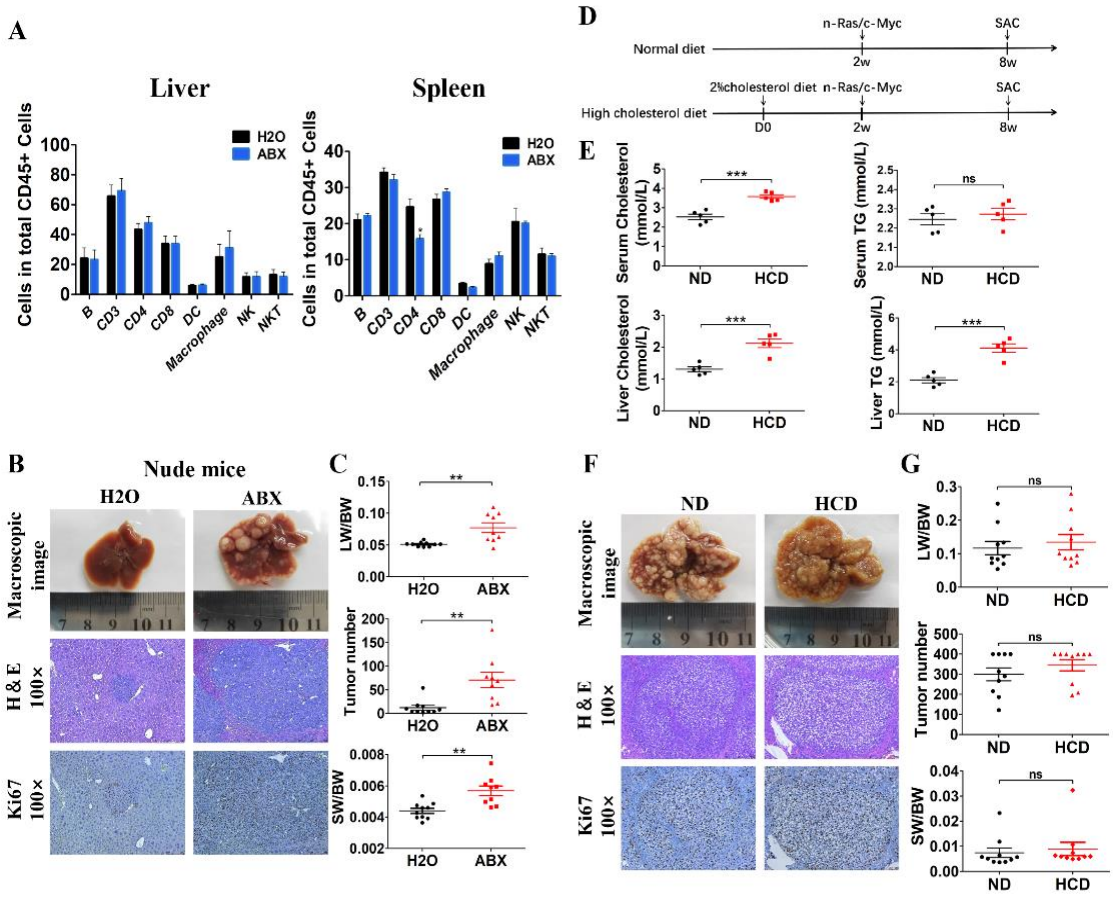

Fig. S6 Antibiotics treatment-induced liver tumor initiation wasn't relevant to immune response and elevated cholesterol level in liver.

(A) After 2 weeks of ABX or H_2O treatment, the relative numbers of immune cells were quantified by flow-cytometric analysis in the liver and spleen (n = 5 per group). (B) Nude mice were transfected with Ras/Myc by HTVi at 2 weeks after the administration of ABX or H_2O and sacrificed 6 weeks after oncogene injection. Representative macroscopic views of livers, H&E staining, and

IHC of Ki67 in nude mouse HCCs. (C) The liver-body weight ratio (LW/BW), tumor number, and the spleen-body weight ratio (SW/BW) of each group (H_2O n = 10; ABX n = 9). (D) Experimental procedure. Mice were transfected with N-Ras/c-Myc by HTVi at 2 weeks after the administration of a High Cholesterol Diet (2% cholesterol, HCD) or a Normal Diet (ND) and mice were sacrificed 4 weeks after oncogene injection. (E) Serum and liver cholesterol and triglyceride levels in mice with HCD or ND before HTVi. (F) Representative macroscopic views of livers, H&E staining, and IHC of Ki67 in mouse HCCs. (G) The liver-body weight ratio (LW/BW), tumor number, and the spleen-body weight ratio (SW/BW) of each group (n = 10 per group). Data was presented as mean ± SEM, *P* values were calculated by Student' s t-test. ns, not significant; ***P* <0.01; ****P* <0.001.

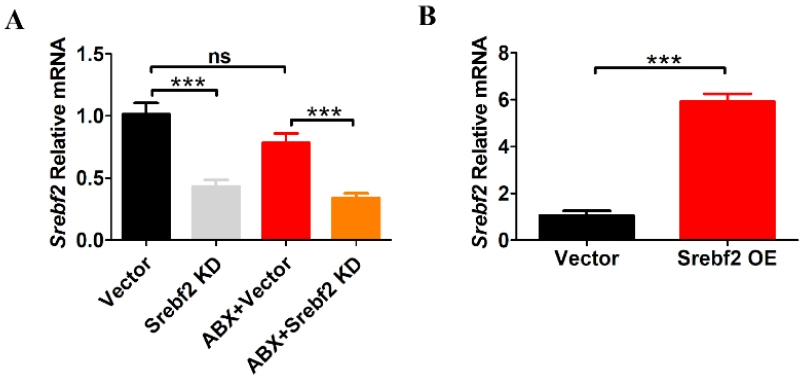

Fig. S7 Validation of AAV8 effect on the expression of liver *Srebf2*.

(A) The AAV8- *Srebf2* KD mediated knockdown of liver *Srebf2* was analyzed using qRT-PCR before HTVi (n = 3 per group). (B) The AAV8- *Srebf2* OE mediated overexpression of liver *Srebf2* was analyzed by qRT-PCR before HTVi (n = 3 per group). Data was presented as mean ± SEM, *P* values were calculated by Student' s t-test. ns, not significant; ****P* <0.001.

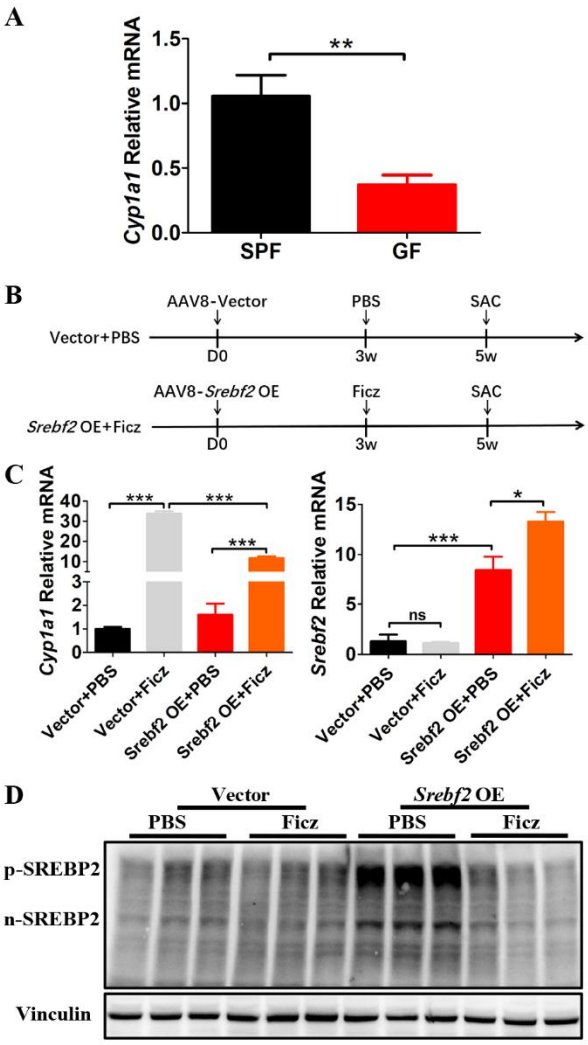

Fig. S8 *Cyp1a1* expression level was inhibited in GF mice, AhR activation inhibited SREBP2 expression under the SREBP2 overexpression condition.

(A) Liver RNA level of *Cyp1a1* in SPF and GF mice were determined using qRT-PCR (n = 5 per group). (B) Experimental procedure. Mice were transfected with AAV8-vector or AAV8-*Srebf2* OE, and Ficz or PBS was intraperitoneally administrated once daily for 14 days at 3 weeks after transfection. Mice were sacrificed after the last administration of PBS or Ficz. (C) Liver RNA levels of *Cyp1a1* and *Srebf2* were determined using qRT-PCR (n = 3 per group). (D) Liver protein levels of liver SREBP2 were determined using western blotting (n = 3 per group). Data was presented as mean ± SEM, *P* values were calculated by Student' s t-test. ns, not significant; **P* <0.05; ***P* <0.01; ****P* <0.001.

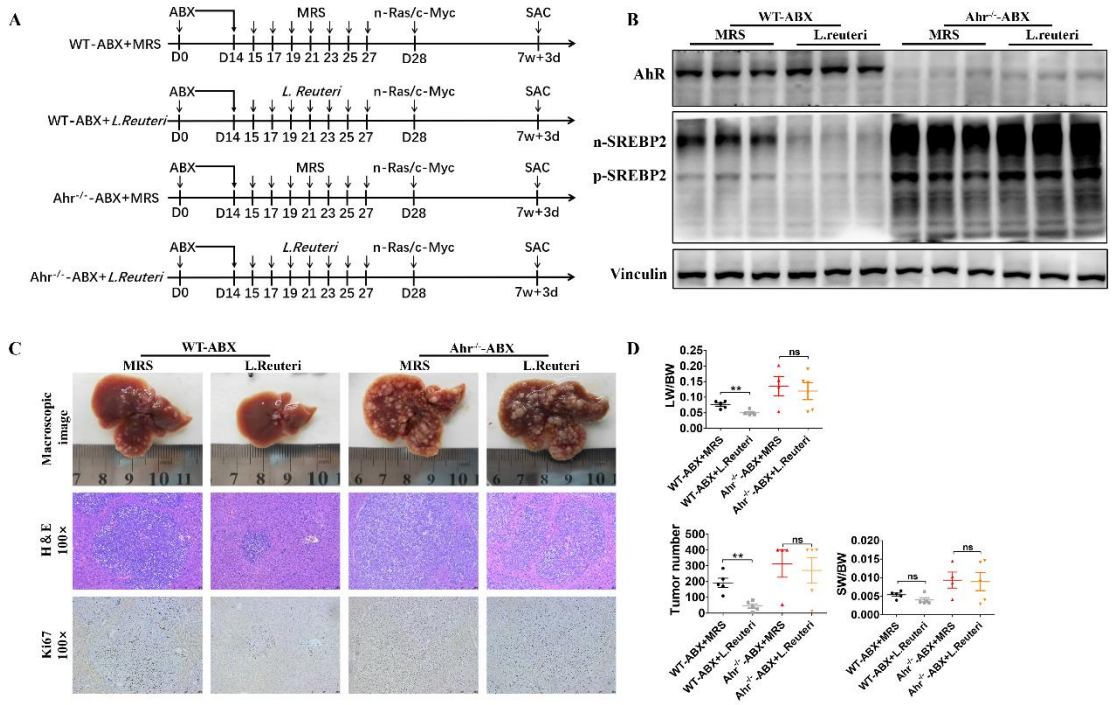

Fig. S9 Supplementation of *Lactobacillus reuteri* failed to inhibit liver SREBP2 expression and liver tumor initiation in *Ahr*$^{-/-}$ mice with gut flora disequilibrium.

(A) Experimental procedure. WT or *Ahr*$^{-/-}$ mice were given *Lactobacillus reuteri* bacteria or lactic acid bacterial culture (MRS) medium every other day after ABX cocktail treatment for 13 days, and 1 day later, HTVi (Ras/Myc) was performed. (B) Levels of AhR and SREBP2 were analyzed using western blotting in livers of WT and *Ahr*$^{-/-}$ mice. (C) Representative macroscopic views of livers, H&E staining, and IHC of Ki67 in mouse HCCs. (D) The liver-body weight ratio (LW/BW), tumor number, and the spleen-body weight ratio (SW/BW) of each group (WT-ABX +MRS n = 5; WT-ABX +*L.Reuteri* n = 5; *Ahr*$^{-/-}$-ABX+MRS n = 4; *Ahr*$^{-/-}$-ABX+*L.Reuteri* n = 5). Data was presented as mean ± SEM, *P* values were calculated by Student' s t-test. ns, not significant; ***P* <0.01.

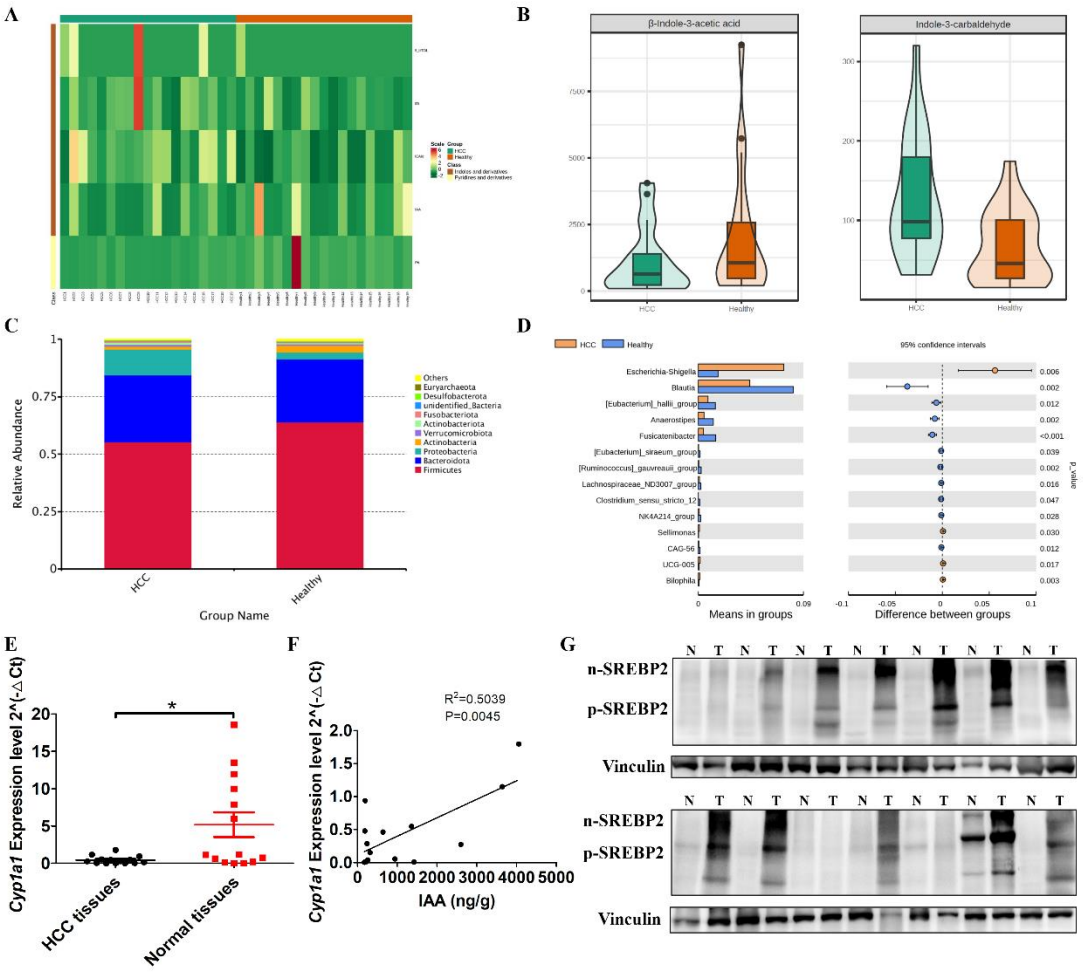

Fig. S10 Fecal tryptophan metabolites and microbiome composition in patients with HCC compared to healthy subjects, reduced AhR activity and increased SREBP2 expression in HCC tissues.

(A) Heatmap showing decreased IAA and increased ICAld in HCC patients compared to healthy subjects (n=19 per group). (B) Violin plot of IAA and ICAld. (C) Beta-diversity comparison at the genus level based on t-test significance results. (D) Beta-diversity comparison at the species level based on t-test significance results. (E) *Cyp1a1* expression level was inhibited in HCC tissues compared to matched adjacent non-tumor tissues. (E) Spearman correlation of the *Cyp1a1* expression level in HCC tissues and fecal IAA levels in HCC patients. (G) SREBP2 expression level was increased in HCC tissues compared to matched adjacent non-tumor tissues. Data was presented as mean ± SEM, *P* values were calculated by paired t-test. **P* <0.05.

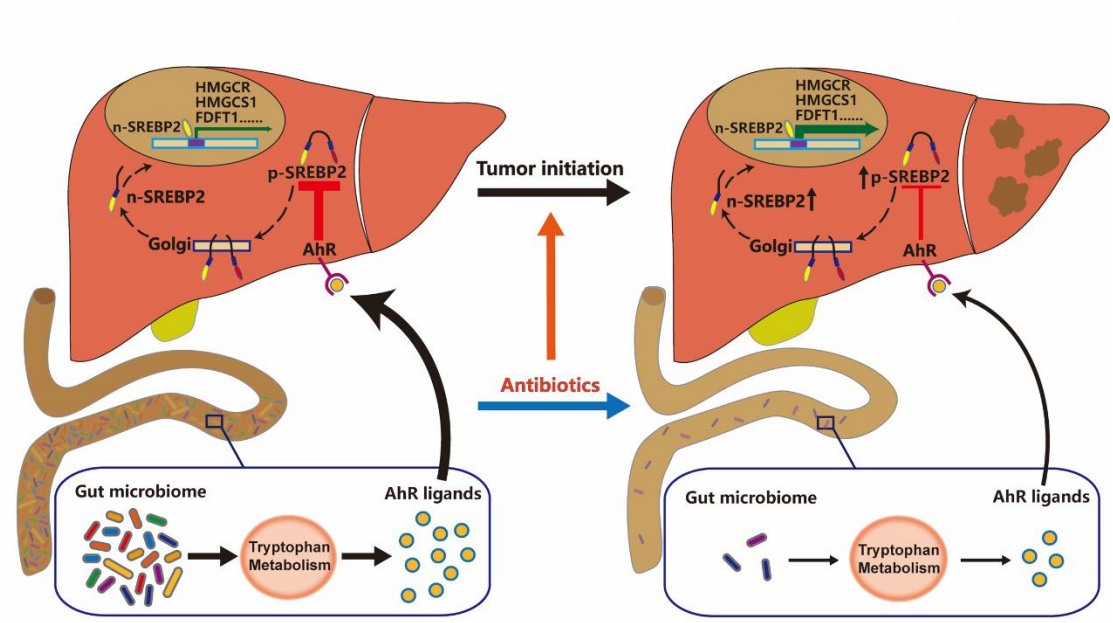

Fig. S11 A schematic diagram showing gut flora disequilibrium promoted liver cancer initiation by modulating gut tryptophan metabolism and upregulating liver SREBP2.

Materials and Methods References

1. Magoc T, Salzberg SL. FLASH: fast length adjustment of short reads to improve genome assemblies. Bioinformatics **2011**;27(21):2957-63 doi 10.1093/bioinformatics/btr507.
2. Haas BJ, Gevers D, Earl AM, Feldgarden M, Ward DV, Giannoukos G, *et al.* Chimeric 16S rRNA sequence formation and detection in Sanger and 454-pyrosequenced PCR amplicons. Genome Res **2011**;21(3):494-504 doi 10.1101/gr.112730.110.
3. Li M, Shao D, Zhou J, Gu J, Qin J, Chen W, *et al.* Signatures within esophageal microbiota with progression of esophageal squamous cell carcinoma. Chin J Cancer Res **2020**;32(6):755-67 doi 10.21147/j.issn.1000-9604.2020.06.09.
4. Chen GY, Zhong W, Zhou Z, Zhang Q. Simultaneous determination of tryptophan and its 31 catabolites in mouse tissues by polarity switching UHPLC-SRM-MS. Anal Chim Acta **2018**;1037:200-10 doi 10.1016/j.aca.2018.02.026.
5. Livak KJ, Schmittgen TD. Analysis of relative gene expression data using real-time quantitative PCR and the 2(-Delta Delta C(T)) Method. Methods **2001**;25(4):402-8 doi 10.1006/meth.2001.1262.